


# Genomic Underpinnings of Population Persistence in Isle Royale Moose

Christopher C. Kyriazis,<sup>\*,1</sup> Annabel C. Beichman,<sup>2</sup> Kristin E. Brzeski,<sup>3</sup> Sarah R. Hoy,<sup>3</sup> Rolf O. Peterson,<sup>3</sup> John A. Vucetich,<sup>3</sup> Leah M. Vucetich,<sup>3</sup> Kirk E. Lohmueller <sup>\*,†,1,4,5</sup> and Robert K. Wayne<sup>\*,†,‡,1</sup>

<sup>1</sup>Department of Ecology and Evolutionary Biology, University of California, Los Angeles, CA

<sup>2</sup>Department of Genome Sciences, University of Washington, Seattle, WA

<sup>3</sup>College of Forest Resources and Environmental Science, Michigan Technological University, Houghton, MI

<sup>4</sup>Interdepartmental Program in Bioinformatics, University of California, Los Angeles, CA

<sup>5</sup>Department of Human Genetics, David Geffen School of Medicine, University of California, Los Angeles, CA

\*Corresponding authors: E-mails: ckyriazis@g.ucla.edu; klohmuller@g.ucla.edu; rwayne@ucla.edu.

†These authors contributed equally to this work.

‡Deceased 26 December 2022.

Associate editor: Rasmus Nielsen

## Abstract

Island ecosystems provide natural laboratories to assess the impacts of isolation on population persistence. However, most studies of persistence have focused on a single species, without comparisons to other organisms they interact with in the ecosystem. The case study of moose and gray wolves on Isle Royale allows for a direct contrast of genetic variation in isolated populations that have experienced dramatically differing population trajectories over the past decade. Whereas the Isle Royale wolf population recently declined nearly to extinction due to severe inbreeding depression, the moose population has thrived and continues to persist, despite having low genetic diversity and being isolated for ~120 years. Here, we examine the patterns of genomic variation underlying the continued persistence of the Isle Royale moose population. We document high levels of inbreeding in the population, roughly as high as the wolf population at the time of its decline. However, inbreeding in the moose population manifests in the form of intermediate-length runs of homozygosity suggestive of historical inbreeding and purging, contrasting with the long runs of homozygosity observed in the smaller wolf population. Using simulations, we confirm that substantial purging has likely occurred in the moose population. However, we also document notable increases in genetic load, which could eventually threaten population viability over the long term. Overall, our results demonstrate a complex relationship between inbreeding, genetic diversity, and population viability that highlights the use of genomic datasets and computational simulation tools for understanding the factors enabling persistence in isolated populations.

**Key words:** *Alces alces*, bottlenecks, genetic load, inbreeding depression, purging.

## Introduction

Anthropogenic habitat fragmentation has dramatically increased the number of isolated and inbred populations (Haddad et al. 2015). To conserve these populations, a crucial question is whether they will be able to persist in isolation, or if they will be driven to extinction by deleterious genetic factors, such as inbreeding depression (Charlesworth and Willis 2009). Numerous examples exist of inbreeding depression driving population decline in isolated populations (Keller and Waller 2002; Hedrick and Garcia-Dorado 2016). However, in some populations, harmful recessive mutations may potentially be “purged” by purifying selection and such purging may avert inbreeding depression (Glémin 2003; Xue et al. 2015; Hedrick and Garcia-Dorado 2016; Robinson et al. 2018; Grossen et al. 2020; Pérez-Pereira et al. 2021). Purging may be most effective in populations where inbreeding is gradual due to

a moderate population size (Day et al. 2003; Glémin 2003; Pekkala et al. 2012; Robinson et al. 2018; Kyriazis et al. 2021; Pérez-Pereira et al. 2021). However, the extent to which purging is a relevant factor for the conservation of threatened populations, and more broadly, the degree to which populations can persist with low genome-wide diversity, is controversial (Ralls et al. 2020; Kardos et al. 2021; Kyriazis et al. 2021; Teixeira and Huber 2021; Kleinman-Ruiz et al. 2022; Pérez-Pereira et al. 2022).

One of the best-studied examples of inbreeding depression driving population decline is the gray wolf population on Isle Royale, an island in Lake Superior roughly 544 km<sup>2</sup> in area. After ~70 years of isolation at a population size generally between ~15 and 30 individuals, the Isle Royale wolf population declined nearly to extinction, with just two individuals remaining in the population in 2018 (Hoy, Peterson, et al. 2020). This population collapse was

© The Author(s) 2023. Published by Oxford University Press on behalf of Society for Molecular Biology and Evolution.

This is an Open Access article distributed under the terms of the Creative Commons Attribution-NonCommercial License (<https://creativecommons.org/licenses/by-nc/4.0/>), which permits non-commercial re-use, distribution, and reproduction in any medium, provided the original work is properly cited. For commercial re-use, please contact [journals.permissions@oup.com](mailto:journals.permissions@oup.com)

Open Access

driven by severe inbreeding depression in the form of widespread congenital deformities (Hedrick et al. 2019; Robinson et al. 2019). The decline of the Isle Royale wolf population has allowed its main prey, moose, to thrive. During the period of the wolf population's decline from 2010 to 2019, the moose population increased from ~500 moose to ~2000 moose (Hoy, Peterson, et al. 2020). The Isle Royale moose population was founded around 1900 likely by a small number of individuals, however the exact circumstances of this founding, and specifically whether it occurred naturally or by humans, remains unknown (Murie 1934; Mech 1966; Sattler et al. 2017). Thus, the Isle Royale moose population has endured in isolation for nearly twice as long as the wolf population and, although some evidence suggests that moose may be able to swim the 24 km distance between the island and nearby mainland, previous genetic studies suggest that the population is genetically isolated from the mainland and has low genetic diversity (Wilson et al. 2003; Sattler et al. 2017). However, despite this long-term isolation and reduced genetic diversity, the moose population appears to be free of obvious signs of inbreeding depression and has similar population growth rates to mainland populations (Hoy, MacNulty, et al. 2020). For instance, 58% of Isle Royale wolves ( $n = 36$ ) were observed to have congenital bone deformities linked to inbreeding (Räikkönen et al. 2009). By contrast, less than 0.5% of Isle Royale moose ( $n > 480$ ) examined over the last decade were observed to have such bone deformities (RO Peterson, unpublished data). Thus, the contrasting fates of the Isle Royale wolf and moose populations provide a compelling case study for understanding the genetic underpinnings of population persistence in isolation.

Outside of the Isle Royale population, North American moose are also known to have low genetic diversity relative to Eurasian moose, which is thought to be a consequence of a relatively recent founder event following the Last Glacial Maximum (Hundertmark et al. 2002, 2003; Decesare et al. 2020). Evidence for this recent founder event also comes from a relative lack of population structure across North America as well as the near absence of moose in the North American fossil record prior to 15,000 years ago (Hundertmark et al. 2002, 2003; Decesare et al. 2020; Dussex et al. 2020). Depending on how recent and severe this founding bottleneck was, the resulting effects of purging may still be apparent in the North American moose population. Thus, the ability of moose to persist in isolation on Isle Royale may be enhanced by purging from historical bottlenecks.

Here, we use a dataset of high-coverage whole-genome sequences from 20 North American moose and 1 Eurasian moose to characterize the impacts of bottlenecks, population isolation, and purging in North American moose, focusing on the Isle Royale population. We confirm previous findings of low genetic diversity in North American moose, especially on Isle Royale, where levels of inbreeding are comparable to that of the Isle Royale wolf population at the time of its decline. Furthermore,

we demonstrate that this low diversity is a consequence of severe founder events in both the North American and Isle Royale populations. Finally, we conduct extensive simulations exploring the impact of bottlenecks and population isolation on genetic load and purging in North American moose. These results suggest substantial purging associated with founding bottlenecks for the North American and Isle Royale populations. Overall, our analysis provides insight into how populations can persist despite severe bottlenecks and high inbreeding and highlights the strengths and limitations of using genomic data to detect purging.

## Results

### Sampling and Population Structure

To examine patterns of moose genetic diversity in North America, we generated a high-coverage whole-genome sequencing dataset for nine moose sampled from Minnesota and seven moose sampled from Isle Royale between 2005 and 2014. We added existing moose genomes to our dataset from Sweden, Alaska, Idaho, Wyoming, and Vermont. These genomes were aligned, genotyped, and annotated relative to the cattle reference genome (ARS-UCD1.2). Although a moose reference genome was recently published (Dussex et al. 2020), we used the more distantly-related cattle reference in order to leverage its fully assembled chromosomes and high-quality annotations (see [Supplementary Material](#) for further discussion). Average sequence coverage after mapping was  $21\times$  (range 11–27; [supplementary table S1, Supplementary Material online](#)).

We first used these data to characterize population structure among North American moose, primarily aiming to assess evidence for isolation of the Isle Royale population. Principal component analysis (PCA) revealed a tight clustering of Isle Royale samples relative to other North American samples, which were distinctly clustered on the first PC ([fig. 1B](#)). However, when down-sampled to one individual per North American population, the Isle Royale and Minnesota samples grouped more closely together, with overall patterns roughly reflecting North American geography ([fig. 1B](#), inset). This suggests that uneven sample sizes may be driving the separation between Isle Royale and Minnesota observed in the full PCA (McVean 2009). Nevertheless, we observe notable differentiation between Isle Royale and Minnesota samples, with a mean  $F_{ST} = 0.083$ . These patterns were also reflected in a tree based on identity-by-state, which found a tight clustering of Isle Royale samples nested within other North American samples and close to Minnesota samples ([fig. 1C](#)). Furthermore, using fastSTRUCTURE analysis, we found no evidence for admixture between Isle Royale and mainland samples ([fig. 1D](#) and [supplementary figs. S1 and S2, Supplementary Material online](#)). Finally, we also estimated kinship for all North American samples, and found that the mainland samples are not closely related to one another

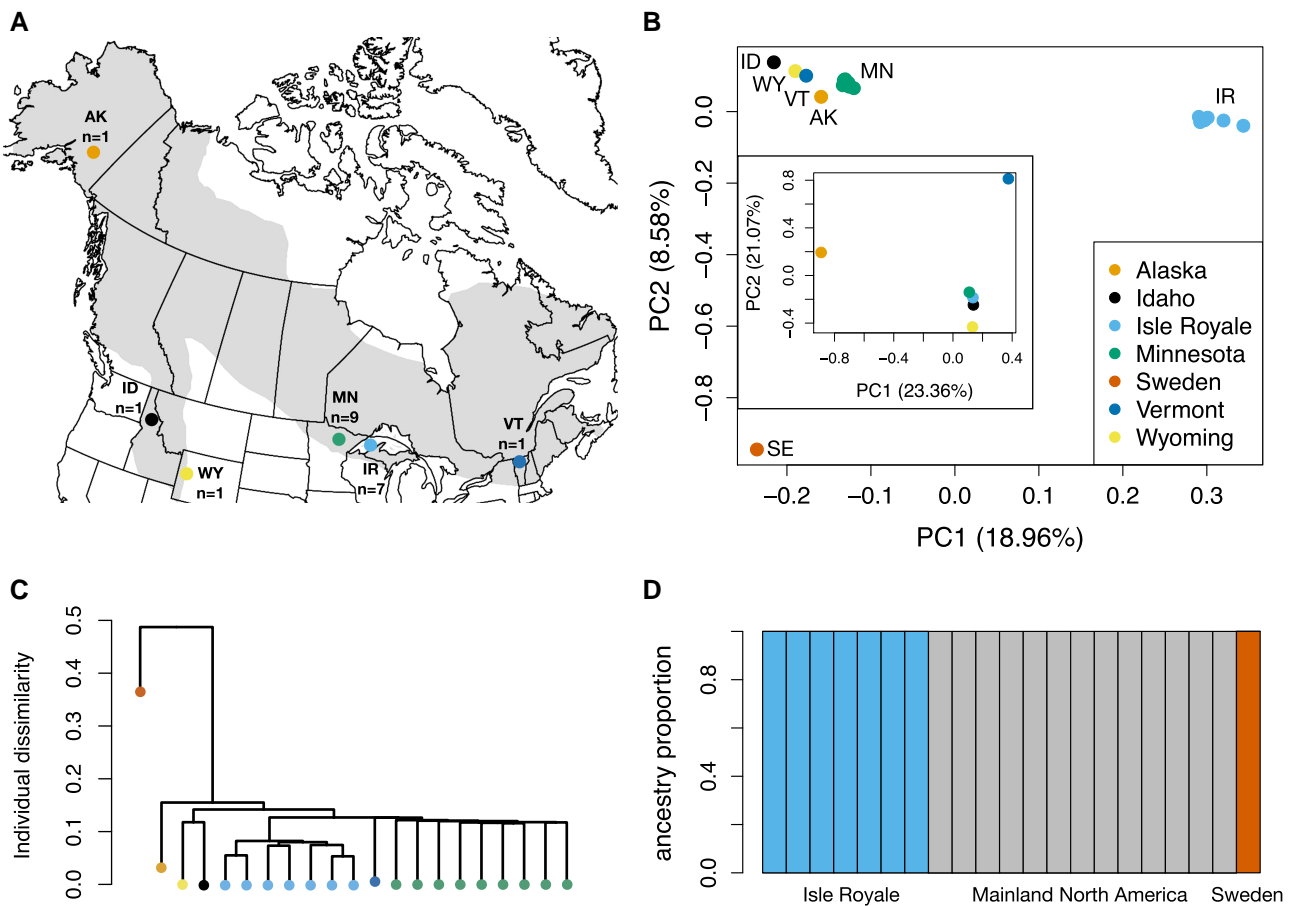


**FIG. 1.** Moose sampling and population structure. (A) Map of North America including localities for individuals sampled for genomic data in our study. Note that Sweden is excluded. (B) PCA of 50,361 LD-pruned SNPs for all sequenced samples. The inset are results when down-sampling to one individual per population and excluding the Swedish sample. (C) Tree based on identity-by-state constructed using 50,361 LD-pruned SNPs. (D) fastSTRUCTURE results for  $K=3$ . See [supplementary figure S1, Supplementary Material](#) online for results with varying  $K$  values and [supplementary figure S2, Supplementary Material](#) online for results when down-sampling to four unrelated individuals each from Isle Royale and Minnesota.

([supplementary fig. S3, Supplementary Material](#) online). However, two pairs of samples from Isle Royale exhibited kinship coefficients consistent with first-order relationships (mean kinship = 0.234; [supplementary fig. S3, Supplementary Material](#) online). In summary, these findings suggest that the Isle Royale population has been isolated from nearby mainland moose populations as suggested by previous work ([Wilson et al. 2003](#); [Sattler et al. 2017](#)) and provide a general characterization of moose population structure in North America.

### Genetic Diversity and Inbreeding

Next, we examined levels of genetic diversity and inbreeding across sampled individuals. Overall, we find that moose have relatively low diversity compared with other mammals ([fig. 2](#)), though these estimates may be slightly downward biased due to using a distant reference genome (see [Supplementary Material](#) for discussion). Additionally, we note that somewhat higher heterozygosity estimates were observed for moose in [Dussex et al. \(2020\)](#) ([fig. 2](#)), likely due to differences in data processing. However, given

that all samples in this study were analyzed using the same bioinformatics pipeline, these issues do not impact estimates of relative diversity across moose populations, where several notable patterns are apparent. First, we observe substantially lower diversity in North American samples relative to a sample from Sweden, with a decrease of at least  $\sim 34\%$  ([fig. 2](#)). This decrease in diversity is likely associated with a founder event for North American moose that is thought to have occurred during the last  $\sim 15,000$  years ([Hundertmark et al. 2002, 2003](#); [Decesare et al. 2020](#)). We observe further reductions in diversity in the Isle Royale population, with an estimated reduction of  $\sim 30\%$  compared with samples from Minnesota ([fig. 2](#)). Surprisingly, we find even lower diversity in mainland samples from Idaho, Wyoming, and Vermont, possibly due to these samples being near the southern range edge, where population densities are generally low and declining ([Timmermann and Rodgers 2017](#); [fig. 2](#)).

Mirroring these patterns of genetic diversity, the impact of inbreeding was prevalent across North American moose genomes in the form of abundant runs of homozygosity (ROH), chromosomal segments that are inherited identical

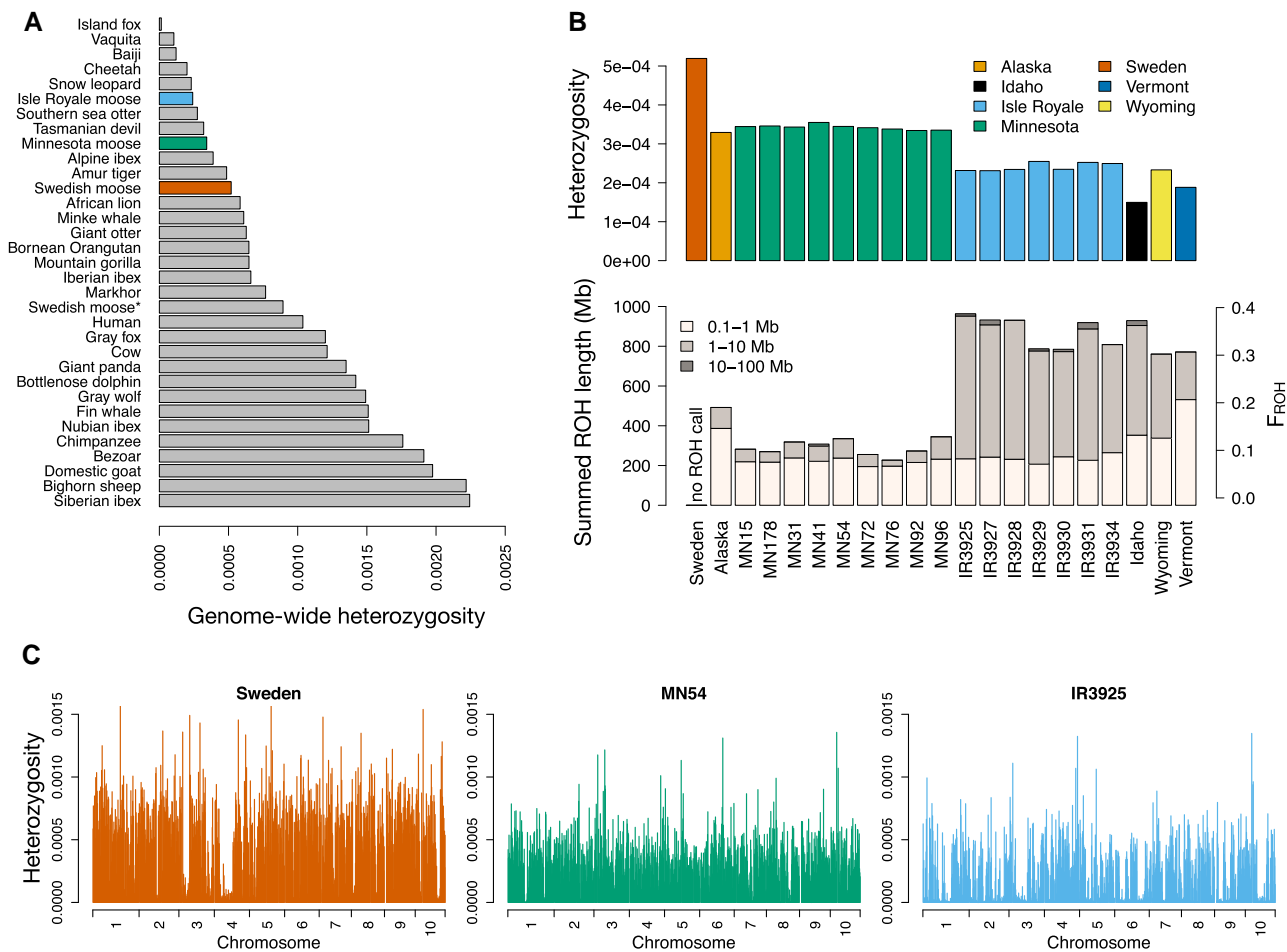


**Fig. 2.** Moose genetic diversity and inbreeding. (A) Comparison of mean genome-wide diversity in three moose populations to published values for other mammals. Note that two estimates are included for the same Swedish moose sample: one from this paper, and a second from [Dussex et al. \(2020\)](#) (denoted with an asterisk), and these estimates differ likely due to differences in bioinformatic pipelines. (B) Plots of mean genome-wide diversity and summed ROH levels for North American moose genomes, with the corresponding  $F_{ROH}$  values on the right-hand axis. Note that we were not able to obtain ROH calls for the Sweden sample due to its differing population origin. (C) Per-site heterozygosity plotted in nonoverlapping 1 Mb windows for representative individuals from Sweden, Minnesota, and Isle Royale. To facilitate visualization, results are plotted only for the first 10 chromosomes. See [supplementary figure S4, Supplementary Material](#) online for plots of all individuals.

by descent from a recent common ancestor ([Kirin et al. 2010](#)). Specifically, we observed high levels of inbreeding in samples from Isle Royale, Vermont, Idaho, and Wyoming, with  $\sim 35\%$  of their autosomal genomes being covered by ROH  $> 100$  kb on average ([fig. 2](#)) and  $\sim 26\%$  covered by ROH  $> 1$  Mb ([supplementary fig. S5, Supplementary Material](#) online). As this fraction represents an estimate of the inbreeding coefficient ( $F_{ROH}$ ), this result suggests that these populations are on average more inbred than an offspring from a full-sib mating ( $F = 0.25$ ). Notably, these levels of inbreeding are comparable to the Isle Royale gray wolf population, where  $\sim 20$ – $50\%$  of their autosomal genomes contained ROH  $> 100$  kb ([Robinson et al. 2019](#)). By contrast, much lower levels of inbreeding were present in samples from Minnesota, Alaska, and Sweden, with  $\sim 12\%$  of these genomes covered by ROH  $> 100$  kb ([fig. 2](#)) and  $\sim 3\%$  covered in ROH  $> 1$  Mb ([supplementary fig. S5, Supplementary Material](#) online).

### Demographic Inference

To understand the demographic processes accounting for these patterns of genetic diversity and inbreeding, we fitted demographic models to the site frequency spectrum (SFS) using *dad*i ([Gutenkunst et al. 2009](#)). Briefly, this approach uses observed allele frequency patterns to estimate demographic parameters for a model with an arbitrary number of population size changes (epochs). Our first aim was to estimate the severity of the North American founding bottleneck, given the apparent impact of this bottleneck on observed differences in genetic diversity between Eurasian and North American moose ([fig. 2](#); [Hundertmark et al. 2002](#)). We generated a folded SFS for our Minnesota samples, and inferred various population size change models including one, two, three, and four-epoch models. Overall, the best-fitting model was a four-epoch model that included two ancestral epochs followed by a severe bottleneck to an effective population size ( $N_e$ )

of 49 for 29 generations and then expansion to  $N_e = 193,472$  for the last 1,179 generations (fig. 3). However, we also found a similar fit for a model with slightly differing bottleneck parameters, suggesting that we have limited power to precisely estimate the duration and magnitude of the bottleneck (supplementary table S2, Supplementary Material online). Nevertheless, both of these models are consistent in detecting a strong bottleneck followed by dramatic population growth taking place  $\sim 1,200$  years ago. The timing of expansion suggests a recent spread of moose across North America starting  $\sim 9,600$  years ago, assuming a generation time of 8 years (Gaillard 2007).

Our next aim for demographic inference was to obtain an estimate of the effective population size of the Isle Royale moose population after its founding  $\sim 120$  years ago using the SFS from our Isle Royale sample. Given the shared evolutionary history of the Minnesota and Isle Royale populations prior to their divergence, we fixed the demographic parameters of our four-epoch model inferred from the Minnesota samples (fig. 3), then added a fifth epoch to this model representing the founding of Isle Royale. Furthermore, we fixed the timing of this fifth epoch to 15 generations ago, thus assuming that the population was founded in the early 1900s (120 years ago assuming a generation time of 8 years; Gaillard 2007), as suggested by available evidence (Murie 1934; Mech 1966). We used this approach to retain power for estimating the Isle Royale effective population size when fitting a complex five-epoch model to a SFS from a small sample of individuals. When fixing these parameters, we obtained an estimate of  $N_e = 187$  on Isle Royale, highlighting a dramatic disparity in  $N_e$  between the North American and Isle Royale populations spanning three orders of magnitude. Additionally, given that the Isle Royale moose population on average numbers  $\sim 1,000$  individuals (Hoy, Peterson, et al. 2020), these results suggest an  $N_e:N$  ratio of  $\sim 0.19$ , consistent with those observed in other species (Frankham 1995). Notably, we observe the same  $N_e:N$  ratio of  $\sim 0.19$  when comparing our estimated North American  $N_e = 193,472$  (fig. 3) to the current census estimate of one million (Timmermann and Rodgers 2017).

### Empirical Patterns of Putatively Deleterious Variation

To understand how the vastly reduced effective population size on Isle Royale may have impacted patterns of deleterious variation compared with mainland populations, we examined variants in protein-coding regions that were predicted to be deleterious and neutral on the basis of evolutionary constraint (Vaser et al. 2016). Specifically, we tested for differences in the derived allele count for synonymous (considered to be putatively neutral), deleterious nonsynonymous, and loss of function (LOF) mutations in the Isle Royale moose genomes relative to the Minnesota genomes. An observed increase in putatively deleterious allele count may be interpreted as evidence for less effective negative selection on Isle Royale, whereas an observed decrease may be interpreted as

purging. We observed minimal changes in allele counts for all categories, including a slight increase in synonymous mutations on Isle Royale of 0.65%, a slight decrease in deleterious nonsynonymous mutations of 0.77%, and a slight increase in LOF mutations of 2.7% ( $P > 0.05$  in all cases by Mann–Whitney  $U$  [MWU] test; fig. 4). Thus, these results do not detect any evidence for fitness declines or purging on Isle Royale.

### Simulations of Deleterious Variation and Genetic Load

Empirical measures of deleterious variation are often challenging to interpret given that the functional impact and dominance of mutations are uncertain (Cooper and Shendure 2011; Pedersen et al. 2017; Kyriazis et al. 2022). Given these limitations, we conducted forward-in-time genetic simulations to assess the impact of bottlenecks on deleterious genetic variation in North American moose using SLiM3 (Haller and Messer 2019). These simulations consisted of a 25 Mb chromosomal segment, which included a combination of introns, exons, and intergenic regions. We modeled deleterious mutations both as nonsynonymous mutations in coding regions using a selection parameter estimated by Kim et al. (2017) as well as noncoding deleterious mutations using parameters estimated by Torgerson et al. (2009) and assumed an inverse relationship between the dominance coefficient of a mutation and its selection coefficient (see Materials and Methods). We assumed a mutation rate of  $7e-9$  per base pair (Dussex et al. 2020) and projected simulated quantities to a 2.5 Gb genome, yielding a deleterious mutation rate of 1.63 per diploid (see Materials and Methods).

Our first aim was to examine the impact of the North American colonization bottleneck on genetic diversity, genetic load, and purging. Here, we define “genetic load” as the realized reduction in fitness due to segregating and fixed deleterious mutations (Kirkpatrick and Jarne 2000) and quantify purging as a reduction in the simulated “inbreeding load”, a measure of the quantity of recessive deleterious variation concealed in heterozygotes (Hedrick and Garcia-Dorado 2016). In other words, the genetic load represents the “realized load” for a population, whereas the inbreeding load represents the “masked load” due to heterozygous recessive deleterious mutations that could potentially be converted into genetic load under future inbreeding (Bertorelle et al. 2022). Here, we report the average change in these quantities across 25 simulation replicates, though note that some variability is present across replicates when simulating at a 25 Mb scale (supplementary fig. S6, Supplementary Material online).

We first investigated dynamics for the North American moose population by simulating under our best-fit demographic model (fig. 3), which includes a founding bottleneck of  $N_e = 49$  for 29 generations followed by expansion to  $N_e = 193,472$  for 1,179 generations. Over the duration of this bottleneck, we observe a decrease in heterozygosity

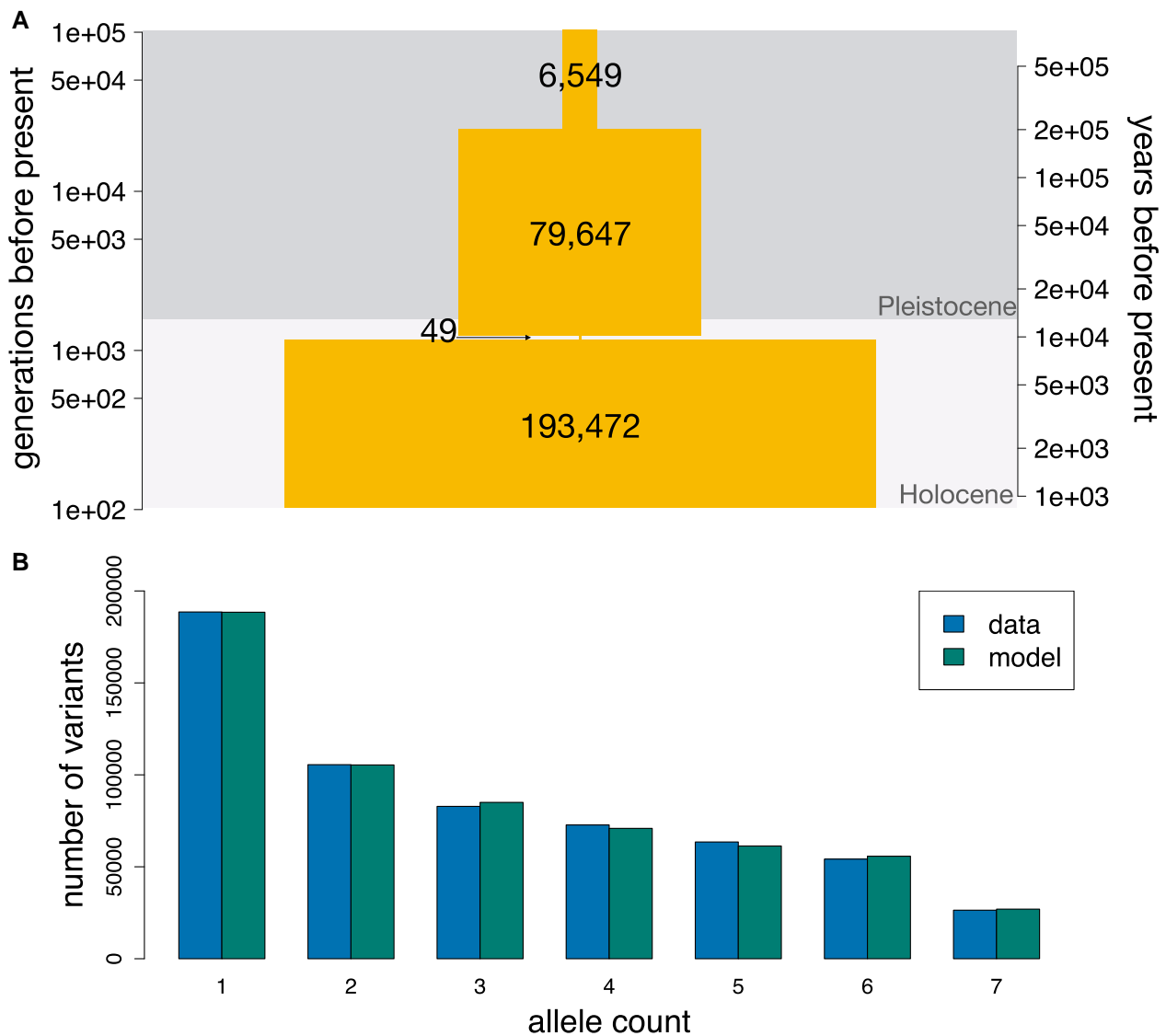


**FIG. 3.** Demographic inference results. (A) Schematic of the best-fit four-epoch model based on the site frequency spectrum (SFS) for the Minnesota sample. The right-hand axis assumes a generation time of 8 years. Numbers denote maximum likelihood estimates of the effective population sizes at various time points. Note the brief and severe bottleneck occurring near the onset of the Holocene. See [supplementary table S2, Supplementary Material](#) online for parameters of the second-best fitting run, which differs somewhat in bottleneck duration and magnitude and pre-/post-bottleneck population sizes. (B) Comparison of the empirical projected folded SFS from the Minnesota sample with the SFS predicted by the model shown in (A).

of 22%, along with a decrease in the inbreeding load of 33% (from  $2B = 7.5$  to  $2B = 5$ ), an increase in genetic load of 27% (from 0.5 to 0.64), and an increase in  $F_{ROH}$  to 0.25 (fig. 5). However, these increases in genetic load and  $F_{ROH}$  are largely absent after 1,179 generations of recovery, though levels of inbreeding notably remain above zero, in agreement with our empirical data (fig. 2B). By contrast, heterozygosity and inbreeding load do not greatly increase after recovery, with the inbreeding load continuing to decline after the bottleneck and remaining 27% below ( $2B = 5.5$ ) its pre-bottleneck value even after 1,179 generations of recovery (fig. 5). Thus, this result suggests that the North American moose population may still be experiencing the lingering purging effects of this founding bottleneck,

despite occurring  $\sim 9,600$  years ago. Importantly, we observe qualitatively similar patterns when simulating under a model with a slightly longer and less severe bottleneck (supplementary fig. S7, Supplementary Material online), suggesting that these simulation results are robust to uncertainty in our estimated demographic parameters. Finally, we also note that this simulated reduction in heterozygosity of 22% is somewhat less than the empirical reduction between North American and Swedish samples of 34% (fig. 2). This may be due to the presence of additional historical bottlenecks in the population that is ancestral to North American moose.

Next, we examined the impact of isolation and small population size for Isle Royale moose on patterns of

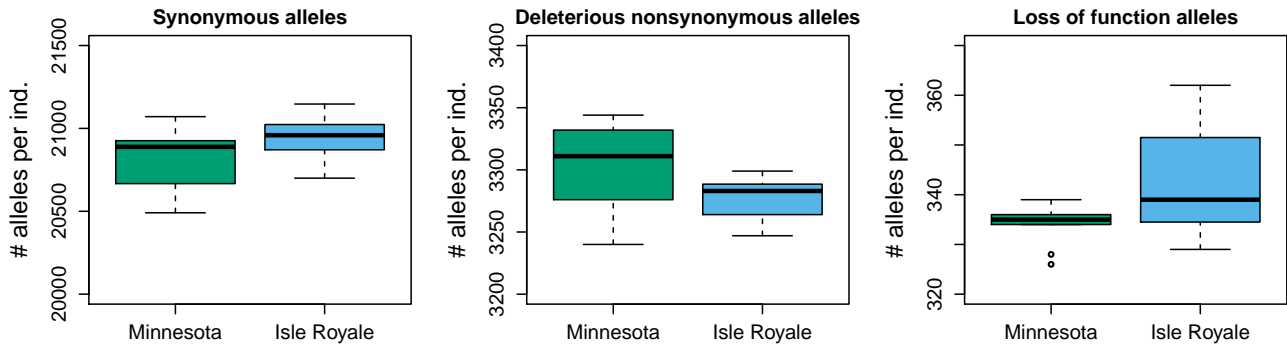


**Fig. 4.** Comparison of derived allele counts between Minnesota and Isle Royale for three mutation types. Synonymous variants are assumed to be putatively neutral, whereas nonsynonymous variants annotated as deleterious or loss of function variants are assumed to be putatively deleterious. Note that no differences in derived allele counts are observed ( $P > 0.05$  in all cases by Mann–Whitney  $U$  test).

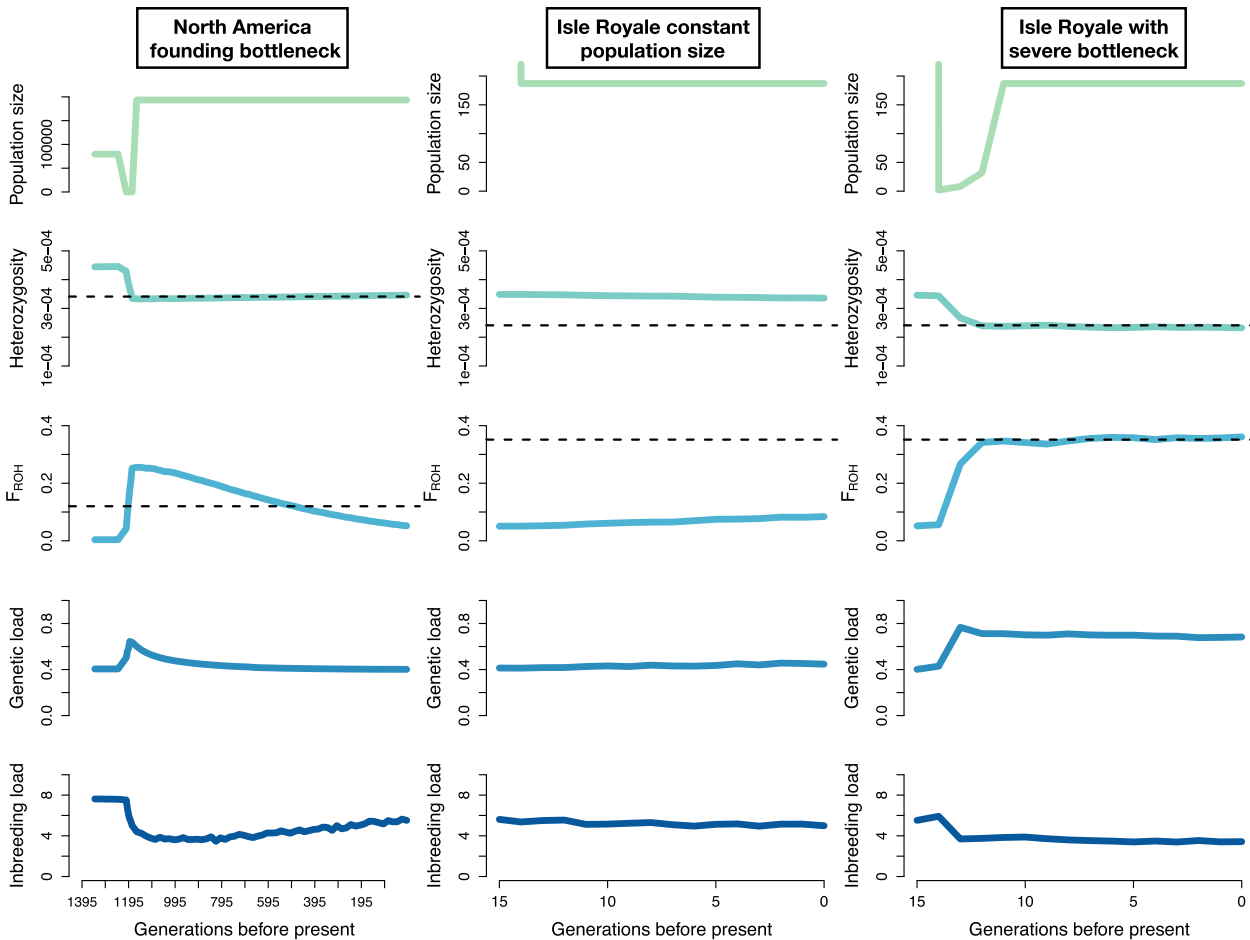


**Fig. 5.** Simulation results under three demographic scenarios. Left column depicts simulation dynamics during the North America founding bottleneck; middle column depicts results when simulating the Isle Royale population at constant population size; right column depicts results when simulating the Isle Royale population including a severe founder event ( $N_e = \{2,8,32\}$  for the first three generations). Each column includes plots of the simulated effective population size, mean heterozygosity, mean levels of inbreeding ( $F_{ROH} > 100$  kb), mean genetic load, and mean inbreeding load from 25 simulation replicates. The dashed lines represent the empirical estimates for heterozygosity and  $F_{ROH}$  from the Minnesota and Isle Royale populations, respectively. Note that the simulation trajectories do not reach these empirical estimates when assuming constant population size (middle column) but do when a founder event is included (right column). See [supplementary figure S6, Supplementary Material](#) online for plots at a 25 Mb scale including all simulation replicates and [supplementary figure S8, Supplementary Material](#) online for results under additional bottleneck parameters.

genetic variation and genetic load. We again simulated under our North America demographic model, though added a final epoch with the estimated Isle Royale demographic parameters of  $N_e = 187$  for 15 generations. When simulating under this demography, however, we do not recapitulate the differences in genetic diversity and inbreeding observed in our empirical data between Isle Royale and mainland samples (fig. 5). Specifically, heterozygosity decreased in the model by only 3.7% compared with a ~30% difference between Minnesota and Isle Royale samples in our empirical data, levels of inbreeding increased only to  $F_{ROH} = 0.08$  compared with  $F_{ROH} = 0.35$  from our empirical data, and  $F_{ST}$  increased only to 0.03, compared with 0.083 in our empirical data (supplementary table S3, Supplementary Material online).

We hypothesized that this discrepancy may be due to the absence of a severe founder event at the origination of the Isle Royale population in our model, given that the population is known to be founded by a small number of individuals (Murie 1934; Mech 1966). To test this hypothesis, we ran simulations where we included a bottleneck during the first three generations following the founding of Isle Royale. We tested three bottleneck severities with effective population sizes during the first three generations of  $N_e = \{6,24,96\}$ ,  $N_e = \{4,16,64\}$ , and  $N_e = \{2,8,32\}$ , each followed by expansion to  $N_e = 187$  for the final 12 generations. These bottleneck parameters were informed by available evidence suggesting that population density was low soon after founding, particularly from 1900 to 1920, though it is unclear exactly how low or how many founders there were (Murie 1934; Mech 1966). When varying these bottleneck parameters, we find that only the most severe bottleneck of  $N_e = \{2,8,32\}$  recapitulated the observed differences in genetic diversity and inbreeding, yielding a decrease in heterozygosity of 33%, an increase in inbreeding to  $F_{ROH} = 0.36$ , and an increase in  $F_{ST}$  to 0.087, in good agreement with our empirical results (fig. 5 and supplementary figs. S8 and S9, Supplementary Material online; supplementary table S3, Supplementary Material online). Moreover, the predicted SFS from models with severe founder events also exhibit better agreement to the empirical Isle Royale SFS compared with a model with no founder event (supplementary fig. S10, Supplementary Material online), further supporting the conclusion that the Isle Royale moose population was founded by very few individuals.

Under this “severe bottleneck model” with two founders, we observe a relative increase in genetic load on Isle Royale of 123% (0.4 to 0.68) as well as a 38% reduction ( $2B = 5.5$  to  $2B = 3.4$ ) in the inbreeding load (fig. 5 and supplementary table S3, Supplementary Material online). Importantly, purging appears to be entirely driven by a reduction in very strongly deleterious alleles ( $s < -0.1$ ) on Isle Royale, which decline from a median of 9.4 to 0 alleles per diploid genome (fig. 6). By contrast, we did not observe significant changes in allele counts for other classes of deleterious mutations (fig. 6). This result may explain why we do not observe a signal of purging in our empirical data

(fig. 4), which likely consists of predominantly weakly or moderately deleterious alleles, given that these alleles are predicted to be by far the most abundant from our model (fig. 6).

To explore sensitivity of these results to the assumed deleterious mutation parameters, we ran simulations under several additional distributions of selection and dominance coefficients while assuming a “severe bottleneck model” for Isle Royale. Overall, we found that our result of substantial purging on Isle Royale accompanied by increases in genetic load was robust to model assumptions, though the exact degree of these changes depends somewhat on selection and dominance parameters (supplementary table S3, Supplementary Material online; supplementary fig. S11, Supplementary Material online). Moreover, we note that our result of substantial purging in the Isle Royale moose population is also found under models with either four or six founding individuals (supplementary table S3, Supplementary Material online; supplementary fig. S8, Supplementary Material online). Thus, the conclusion that purging has likely occurred in the Isle Royale moose population is supported by a wide array of model parameterizations.

Finally, we explored the potential impact of a low rate of historical migration on genetic diversity, genetic load, levels of inbreeding, and inbreeding load in the Isle Royale population. We ran simulations under a “severe bottleneck model” with migration fractions of 0.5% and 5%, roughly corresponding to 1 and 10 effective migrants per generation, respectively, chosen to model two relatively low but plausible rates of migration. Under the low migration scenario of 0.5%, results are nearly identical to the no migration scenario (supplementary fig. S12, Supplementary Material online; supplementary table S3, Supplementary Material online), implying that a very low level of historical migration (~1 migrant per generation) would not have had much impact on the genetic state of the population. These results imply that we cannot fully rule out the possibility of a low rate of migration to Isle Royale, as suggested by direct observations of moose swimming between Isle Royale and the mainland (Vucetich 2021). By contrast, when the migration fraction is increased to 5%, heterozygosity is higher and inbreeding lower relative to empirical values (supplementary fig. S12, Supplementary Material online; supplementary table S3, Supplementary Material online). Together, these results suggest that historical migration to Isle Royale was either absent or very low. Moreover, these results also imply that any future attempts to restore genetic diversity and reduce genetic load in the Isle Royale moose population would require a relatively high rate of migration (>10 effective migrants per generation).

## Discussion

Highly inbred populations are often thought to be doomed to extinction. However, some can persist, and understanding the factors enabling persistence can aid in



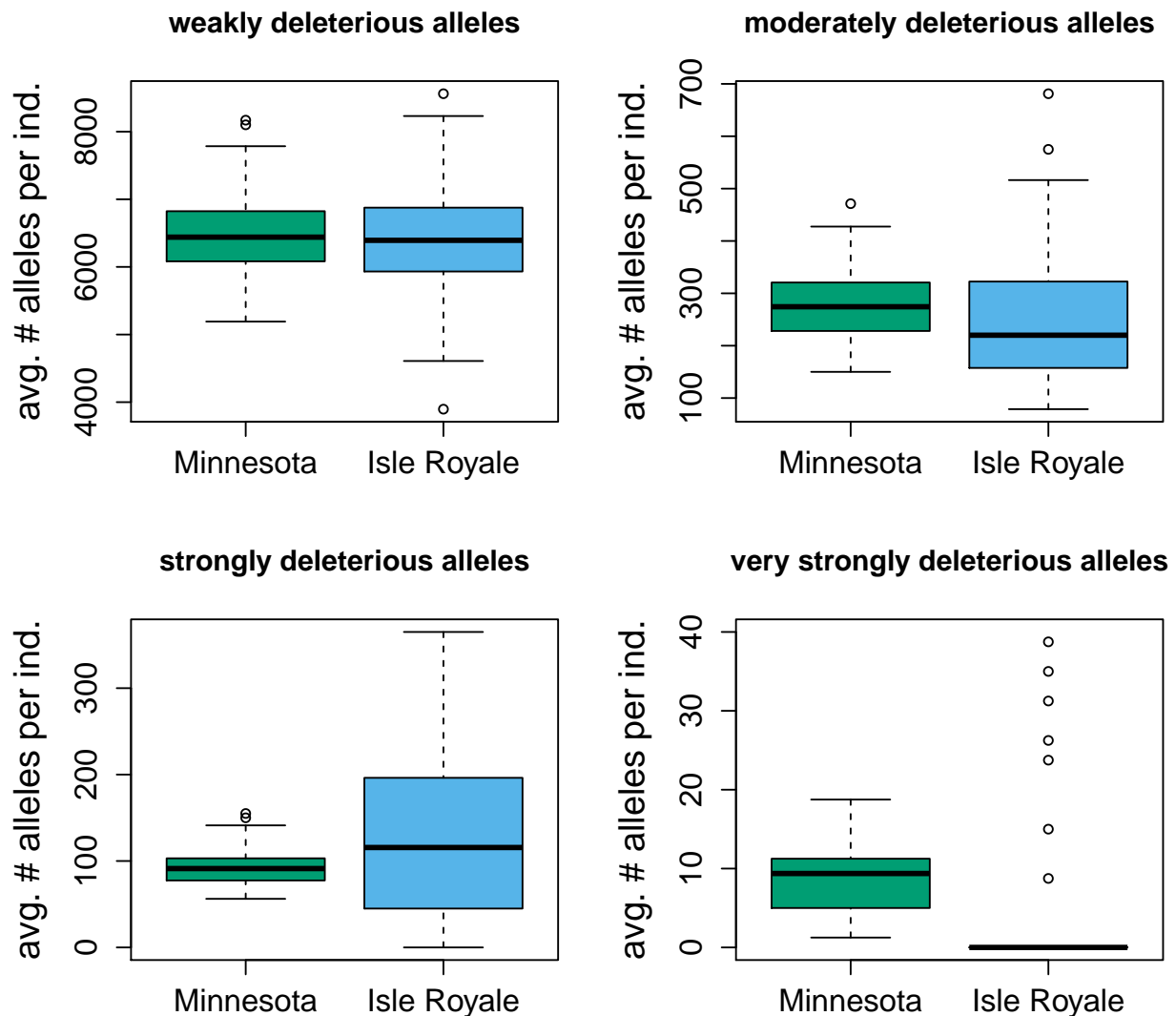


**FIG. 6.** Comparison of genome-wide deleterious allele counts for simulated mainland and Isle Royale populations assuming a severe founder event scenario. Allele counts for the Isle Royale population were recorded at the conclusion of 15 simulated generations. We define weakly deleterious alleles as mutations with  $s > -0.001$ , moderately deleterious alleles as  $-0.01 \leq s < -0.001$ , strongly deleterious alleles as  $-0.1 \leq s < -0.01$ , and very strongly deleterious alleles as  $s < -0.1$ . Note that differences in allele counts are only present for the rare category of very strongly deleterious mutations. Also, note that the variance for allele counts is over-dispersed relative to expectation for a full 2.5 Gb genome given that results are projected from simulation results for a 25 Mb chromosomal segment.

conservation efforts. Our results document high inbreeding in the Isle Royale moose population ( $F_{ROH} = 0.35$  on average; [fig. 2](#)), roughly as high as that observed in the gray wolf population at the time of its decline. Yet, despite these high levels of inbreeding, the Isle Royale moose population appears to be free of obvious signs of inbreeding depression, unlike the wolf population ([Räikkönen et al. 2009](#); [Robinson et al. 2019](#)). A key factor likely underlying these differences is the history of inbreeding in these populations. Whereas the wolf population became severely inbred due to many generations of near-complete isolation at a population size of  $\sim 15$ – $30$  individuals ([Hedrick et al. 2019](#); [Robinson et al. 2019](#)), the moose population has largely avoided close inbreeding for most of its history on the island due to having a much larger population size. Although the moose population experienced a brief period

of very small population size during a severe founder event, our analyses suggest the population rapidly grew to a more moderate size ( $N_e = 187$ ). Additionally, historical bottlenecks in the North American moose population may have also lowered levels of segregating recessive deleterious variation compared with those present in the wolf population, which may also help explain the varying degrees of inbreeding depression observed in each population. Finally, the breeding system of wolves may also contribute to elevated inbreeding in the wolf population, given that wolves live in territorial packs where only a few individuals reproduce.

The differing demographic histories and reproductive systems of the Isle Royale wolf and moose populations are reflected in the distribution of ROH lengths observed in each population. In the wolf population, ROH were predominantly long ( $>10$  Mb), reflecting recent and severe

inbreeding (Robinson et al. 2019), whereas the moose population exhibits an abundance of intermediate-length ROH (1–10 Mb; fig. 2). Several recent studies have highlighted the severe fitness consequences of long ROH, which tend to be enriched for highly deleterious recessive alleles, whereas more intermediate-length ROH may be largely purged of such variation (Szpiech et al. 2013, 2019; Robinson et al. 2019; Stoffel et al. 2021a; Swinford et al. 2022). Thus, these results suggest that purging may have facilitated persistence in the Isle Royale moose population.

Our simulation results provide further support for the conclusion that purging has occurred in the Isle Royale moose population. Under a variety of plausible genetic and demographic parameters, we observe substantial 30–68% reductions in the simulated inbreeding load (supplementary table S3, Supplementary Material online), with the “severe bottleneck model” suggesting a reduction of 38% (fig. 5). When projecting this inbreeding load genome-wide, the total inbreeding load predicted by our model is  $2B = 3.4$  for the Isle Royale moose population, much lower than an estimate of the vertebrate median of  $2B = 4.5$  (Nietlisbach et al. 2019). Somewhat surprisingly, however, we find that inbreeding and purging in the Isle Royale moose population appears to have been largely driven by a severe founder event, with minimal changes in genetic diversity, levels of inbreeding, or load occurring during the ~12–15 generations of persistence at moderate population size (fig. 5). Thus, these results imply that even relatively prolonged persistence (~120 years or ~15 generations) at moderate population size ( $N_e = 187$ ) is not by itself sufficient to result in substantial purging or decrease in neutral heterozygosity. Importantly, this result does not imply that purging would not take place over the much longer term (i.e., hundreds of generations or thousands of years) at such population sizes, as has been documented in several species (Xue et al. 2015; Robinson et al. 2018, 2022; Pérez-Pereira et al. 2021). Indeed, such gradual purging over longer timescales remains ideal for isolated populations, as it would not concomitantly elevate genetic load. Thus, we emphasize that our results do not advocate for inducing severe bottlenecks in natural populations to facilitate purging, as there may be many negative consequences of such bottlenecks. Instead, maintaining isolated populations at moderate sizes ( $N_e > 100$ ) that are large enough to avoid close inbreeding appears to be a better approach for ensuring viability over the short to intermediate term. Finally, our simulations also suggest that purging in the Isle Royale moose population is almost entirely driven by a reduction in very strongly deleterious alleles ( $s < -0.1$ ), with no evidence for changes in derived allele counts for deleterious mutations of more modest effect (fig. 6). Such highly deleterious mutations are known to be most susceptible to purging, both due to high strength of negative selection operating against them and their propensity to be lost by genetic drift due to their rarity (Hedrick 1994; Wang et al. 1999; Kyriazis et al. 2021).

The fact that we do not observe any reductions in allele frequency for deleterious mutations of more modest effect

( $s > -0.1$ ) in our simulations likely explains why we do not detect a signal of purging in our genomic dataset (fig. 4). Specifically, deleterious mutations with  $s > -0.1$  comprise the overwhelming majority of segregating deleterious mutations in our simulations, with only nine highly deleterious mutations ( $s < -0.1$ ) predicted to be segregating in the Minnesota moose population by our simulations out of a total of 6,787 segregating deleterious mutations (fig. 4). Although our simulation results demonstrate a significant purging of these highly deleterious mutations, our empirical analysis is unable to detect this signal given that these mutations are extremely rare and challenging to identify in genomic sequencing data. This challenge of identifying highly deleterious variants in genomic variation datasets is perhaps exemplified by LOF mutations, a class of mutations that may be expected to be highly deleterious, though in reality often have only modest effects on fitness (MacArthur and Tyler-Smith 2010; MacArthur et al. 2012; Cassa et al. 2017; Agarwal et al. 2022). For instance, in humans, often  $>100$  LOF mutations are observed in healthy individuals, questioning the assumption that such mutations are always highly deleterious (MacArthur and Tyler-Smith 2010; MacArthur et al. 2012). Moreover, understanding whether such mutations are recessive also presents a major challenge that has yet to be overcome even in humans (Cassa et al. 2017; Fuller et al. 2019; Agarwal et al. 2022). This challenge of knowing the dominance coefficient for putatively deleterious mutations may also limit our ability to detect elevated genetic load. For instance, although we did not observe evidence for elevated genetic load in the Isle Royale moose population in the form of an increased burden of derived deleterious alleles (fig. 4), our simulation results suggest that genetic load may in fact be much higher in the Isle Royale population (fig. 5 and supplementary table S3, Supplementary Material online). This discrepancy is due to the effects of recessive deleterious mutations being ignored in a comparison of derived allele counts for putatively deleterious variation, as the dominance coefficients of such mutations remain unknown. Thus, these considerations highlight a major limitation of quantifying genetic load and purging using genomic sequencing datasets, given that available methods for detecting putatively deleterious variation are unable to reliably predict  $s$  and  $h$  for individual mutations (Huber et al. 2020; Kyriazis et al. 2022; Sandell and Sharp 2022; Robinson et al. 2023).

Another limitation of our analysis is that we are unable to validate our findings using field observations comparing individual fitness and levels of inbreeding (e.g., Stoffel et al. 2021b). Such data are not available for the vast majority of wild populations, including the Isle Royale moose population. Given this limitation, our study highlights the utility of simulation modeling for aiding in interpreting patterns of variation present in genomic datasets and quantifying purging and genetic load building on previous studies (Arunkumar et al. 2015; Xue et al. 2015; Robinson et al. 2018, 2022; Grossen et al. 2020; Dussex et al. 2021; Khan et al. 2021; Kleinman-Ruiz et al. 2022). One major benefit

of our extensive simulation analysis is that it allows us to explore which historical demographic events (e.g., founder events, migration, etc.) are consistent with patterns observed in our genomic variation dataset, and which specific factors are responsible for driving purging. Further validation of such approaches using field-based data represents a key area for future research.

Our findings also have important implications for understanding the evolutionary history and conservation status of mainland North American moose populations. Across all North American moose samples, we observe a reduction in genome-wide diversity of at least 34% relative to a sample from Sweden (fig. 2), consistent with previous work (Hundertmark et al. 2002; Dussex et al. 2020). Our demographic modeling indicates this reduction in diversity is largely due to a severe bottleneck in the ancestral North American moose population occurring ~9,600 years ago (fig. 3). This timing closely aligns with glacial recession at the onset of the Holocene 11,000 years ago as well as the North American fossil record (Decesare et al. 2020). Furthermore, our simulation results suggest a substantial 34% purging of the inbreeding load associated with this founding bottleneck, the effects of which may persist until the present day (fig. 5). This phenomenon could further explain the continued persistence of the isolated Isle Royale moose population, implying that the founding individuals may have been somewhat “pre-purged” of inbreeding depression. These factors could also help explain the success of other introduced moose populations in North America, such as the Newfoundland population, which was founded by just six individuals and now numbers >100,000 individuals (Broders et al. 1999). Nevertheless, many fragmented North American moose populations near the southern range edge have experienced recent declines (Timmermann and Rodgers 2017). Though these declines have generally been linked to synergistic impacts of climate change and increasing disease and pathogen load (Murray et al. 2006; Timmermann and Rodgers 2017), the potential role of genetic factors has been largely overlooked. For example, we observed low genetic diversity in samples from Idaho and Wyoming (fig. 2), perhaps due to the recent founding of these populations in the mid-19th century and low population density (Wolfe et al. 2010). Notably, moose in this region exhibit low adult pregnancy rates (Ruprecht et al. 2016), which could potentially be a consequence of inbreeding depression. Moreover, it is possible that low genetic diversity in these populations has increased their susceptibility to parasites (Gibson and Nguyen 2021). Overall, the causes of moose population declines near the southern range edge appear to be complex, and additional genomic sampling of these populations will be necessary to more fully investigate the potential role of genetic factors.

In conclusion, our results depict a complex relationship between genetic diversity, inbreeding, and population viability in isolated and fragmented populations. Whereas the wolf population declined nearly to extinction due to having an extremely small  $N_e < 10$  (Adams et al. 2011), the

moose population continues to persist in part due to its much larger  $N_e$  of ~200 for most of its history after the initial founding. Moreover, this case study of predator and prey hints at a more far-reaching phenomenon, in which isolated predator populations may face an elevated extinction risk due to inbreeding depression as a result of their naturally lower density, whereas the higher abundance of prey populations may enable them to evade the most severe impacts of inbreeding depression. In light of the well-documented connections among gray wolf, moose and plant abundance on Isle Royale (McLaren and Peterson 1994), these results suggest the possibility of an eco-evolutionary link between purging and the dynamics of the Isle Royale ecosystem. In general, purging may have system-wide effects in other isolated and fragmented ecosystems, where predator populations are declining in part due to inbreeding depression, and prey populations are thriving in their absence, often to the detriment of the broader ecosystem (Estes et al. 2011; Ripple et al. 2014). Thus, our results highlight a unique connection between deleterious genetic variation and ecosystem health, with implications for best management practices of small and fragmented populations.

## Materials and Methods

### Sampling and Sequencing

Isle Royale tissue samples were obtained opportunistically from moose carcasses and frozen and archived at MTU. Minnesota tissue samples were collected during regular management activities and frozen and archived by the Department of Natural Resources. DNA was extracted from samples using Qiagen kits and quantified using a Qubit fluorometer. Whole-genome sequencing was performed on an Illumina NovaSeq at the Vincent J. Coates Genomics Sequencing Laboratory at University of California, Berkeley and MedGenome. Existing genomes from Kalbfleisch et al. (2018) and Dussex et al. (2020) were downloaded from the National Center for Biotechnology Information (NCBI) Sequence Read Archive (see supplementary table S1, Supplementary Material online).

### Read Processing and Alignment

We processed raw reads using a pipeline adapted from the Genome Analysis Toolkit (GATK) (Van der Auwera et al. 2013) Best Practices Guide. We aligned paired-end 150 bp raw sequence reads to the cattle genome (ARS-UCD1.2) using BWA-MEM (Li 2013), followed by removal of low-quality reads and PCR duplicates. Given that we do not have a database of known variants, we did not carry out Base Quality Score Recalibration, but instead carried out hard filtering of genotypes (see below). Although the cattle genome is highly divergent from moose, we opted to use it due to its much higher quality and contiguity compared with existing moose genomes (scaffold N50 of 103 Mb for ARS-UCD1.2 vs. 1.7 Mb for

NRM\_Aalces\_1\_0). In addition, high-quality annotations exist for the cattle genome, including existing resources on the Ensembl Variant Effect Predictor database (McLaren et al. 2016), whereas available moose genomes are not annotated. To explore the potential impact of using a distant reference genome on downstream analyses, we mapped a subset of 10 samples to an existing moose reference genome (NRM\_Aalces\_1\_0) as well as a hog deer reference genome (ASM379854v1) that is somewhat less divergent than cattle, but has lower contiguity (scaffold N50 of 20.7 Mb). Importantly, we found that the choice of reference genome here has a relatively minor impact on genetic diversity and runs of homozygosity. Thus, we use the cattle reference genome for all downstream analyses (see [Supplementary Material](#) for further discussion).

### Genotype Calling and Filtering

We performed joint genotype calling at all sites (including invariant sites) using GATK HaplotypeCaller. Genotypes were filtered to include only high-quality biallelic SNPs and monomorphic sites, removing sites with Phred score below 30 and depth exceeding the 99th percentile of total depth across samples. In addition, we removed sites that failed slightly modified GATK hard filtering recommendations ( $QD < 4.0$  ||  $FS > 12.0$  ||  $MQ < 40.0$  ||  $MQRankSum < -12.5$  ||  $ReadPosRankSum < -8.0$  ||  $SOR > 3.0$ ), as well as those with  $>25\%$  of genotypes missing or  $>35\%$  of genotypes heterozygous. We masked repetitive regions using a mask file downloaded from [https://www.ncbi.nlm.nih.gov/assembly/GCF\\_002263795.1/](https://www.ncbi.nlm.nih.gov/assembly/GCF_002263795.1/). Finally, we applied a per-individual excess depth filter, removing genotypes exceeding the 99th percentile of depth for each individual, as well as a minimum depth filter of six reads.

### Population Structure and Relatedness

We used SNPrelate v1.14 (Zheng et al. 2012) to run principal component analysis (PCA), construct a tree based on identity-by-state (IBS), and estimate kinship among sampled genomes. For these analyses, we pruned SNPs for linkage disequilibrium ( $ld.threshold = 0.2$ ) and filtered out sites with minor allele frequency below 0.05, resulting in 50,361 SNPs for analysis. PCA was run both for all sampled individuals as well as for North American individuals down-sampled to one individual per population. We used the KING method of moments approach (Manichaikul et al. 2010) to estimate kinship among North American moose samples. Finally, we estimated IBS among all samples, then performed hierarchical clustering on the resulting matrix to construct a dendrogram.

As another means of characterizing population structure, we used fastSTRUCTURE v1.0 (Raj et al. 2014) to test for admixture among sampled individuals. We converted our vcf to PLINK bed format, retaining variants with a minor allele frequency of at least 0.05 and maintained the order of alleles from the original vcf file. We ran fastSTRUCTURE on all sampled individuals as well as

only Minnesota and Isle Royale individuals, each down-sampled to five unrelated individuals. For both analyses, we ran fastSTRUCTURE using values of  $k$  from 1 to 4. Finally, we used vcftools (Danecek et al. 2011) to estimate Weir and Cockerham's (Weir and Cockerham 1984)  $F_{ST}$  between all Minnesota and Isle Royale samples using default settings.

### Genetic Diversity and Runs of Homozygosity

We calculated heterozygosity for each individual in non-overlapping 1 Mb windows across the autosomal genome. We removed windows with fewer than 80% of sites called, as well as windows below the 5th percentile of the total number of calls, as these windows have high variance in heterozygosity. We estimated mean genome-wide heterozygosity by averaging heterozygosity across windows for each individual.

Runs of homozygosity were called using BCFtools/ROH (Narasimhan et al. 2016). We used the -G30 flag and allowed BCFtools to estimate allele frequencies. Due to the Swedish sample coming from a highly divergent population with differing allele frequencies, we excluded it from this analysis. We used a custom R script (R Core Team 2021) to partition the resulting ROH calls into length categories 0.1–1 Mb, 1–10 Mb, and 10–100 Mb. We calculated  $F_{ROH}$  by summing the total length of all ROH calls  $>100$  kb (or  $>1$  Mb) and dividing by 2,489.4 Mb, the autosomal genome length for the cattle reference genome. When conducting this analysis for the subset of samples mapped to the hog deer reference genome, we only used scaffolds  $>1$  Mb in length, which together sum to 2,479 Mb ( $\sim 93\%$  of the total reference length). Similarly, when conducting this analysis with samples mapped to the moose genome, we also restricted our analysis to scaffolds  $>1$  Mb in length, comprising 1,804 Mb ( $\sim 73\%$  of the total reference length).

### Identifying Putatively Deleterious Variation

Variant sites were annotated using the Ensembl Variant Effect Predictor (VEP) v.97 (McLaren et al. 2016). We used SIFT (Vaser et al. 2016) to identify synonymous, deleterious nonsynonymous, and loss of function variants and compare derived allele counts between our Minnesota and Isle Royale samples. Here, we use synonymous variants as a proxy for neutral variants within coding regions to serve as a comparison for two classes of putatively deleterious variation. Whereas average derived allele counts for putatively neutral synonymous variants are not expected to differ between populations with differing demographic histories, derived allele counts for putatively deleterious variants may differ due to differences in the strength of negative selection (Simons et al. 2014). We defined deleterious nonsynonymous variants as those having a SIFT score  $<0.05$  and loss of function variants as those that disrupted splice sites, start codons, or stop codons. For each category of mutations, we tallied the number of derived alleles relative to the cow reference, comparing these tallies for genomes

sampled from Isle Royale and Minnesota to assess whether any differences in derived deleterious allele counts may be present due to small population size on Isle Royale. Variants that were fixed derived across the entire sample were not included.

### Demographic Inference

We estimated historical demographic parameters for North American moose based on the neutral site frequency spectrum (SFS) using *∂a∂i* (Gutenkunst et al. 2009). In brief, we first focused on estimating parameters for the mainland North American population based on the neutral SFS for our nine Minnesota genomes, then used these results to guide inference of the effective population size on Isle Royale based on a neutral SFS from five genomes of unrelated Isle Royale individuals.

To generate a neutral SFS, we began by identifying regions that were >10 kb from coding regions and did not overlap with repetitive regions. We also excluded unannotated highly conserved regions that are under strong evolutionary constraint, identified by aligning the remaining regions against the zebra fish genome using BLASTv2.7.1 (Camacho et al. 2009) and removing any region which had a hit above a 1e-10 threshold. We then generated a folded neutral SFS for these regions using a modified version of EasySFS (<https://github.com/isaacovercast/easySFS>), which implements *∂a∂i*'s hypergeometric projection to account for missing genotypes. We found that the number of SNPs was maximized by using a projection value of seven diploids for the Minnesota sample and four diploids for the Isle Royale sample. In addition, we counted the number of monomorphic sites passing the projection threshold in neutral regions and added these to the 0 bin of the SFS.

We used these SFSs to conduct demographic inference using the diffusion approximation approach implemented in *∂a∂i* (Gutenkunst et al. 2009). Using the Minnesota SFS, we fit 1-epoch, 2-epoch, 3-epoch, and 4-epoch models. These models included the following parameters:  $N_{anc}$  (the ancestral effective population size),  $N_{1-3}$  (the effective size of the subsequent 1–3 epochs), and  $T_{1-3}$  (the duration of the subsequent 1–3 epochs; [supplementary table S2, Supplementary Material](#) online). In other words, a 3-epoch model includes the parameters  $N_{anc}$ ,  $N_1$ ,  $N_2$ ,  $T_1$ , and  $T_2$ . Overall, we found the best fit for a 4-epoch model including expansion in the second epoch followed by a strong bottleneck and a final epoch of expansion, though with poor convergence of estimated parameters. Based on initial results, we constrained parameter space for the 4-epoch model by setting a limit on  $N_1$  to be in the range  $[10, 30] * N_{anc}$ ,  $N_2$  to be in the range  $[1e-2, 5] * N_{anc}$ , and  $N_3$  to be in the range  $[10, 40] * N_{anc}$ .

We next sought to obtain an estimate of the effective population size on Isle Royale using a folded neutral SFS from five unrelated individuals, projected to four diploids. Given this limited sample size and the shared evolutionary history of Isle Royale and Minnesota moose, we fixed the

parameters estimated from our 4-epoch model inferred above based on the Minnesota SFS. We then added a fifth epoch to the model, fixing the duration of this epoch to 15 generations, based on an estimated date of colonization of 1900 and 8-year generation time (Gaillard 2007). Thus, the only estimated parameter in this approach is  $N_s$ , the effective population size on Isle Royale.

We carried out inference by permuting the starting parameter values and conducting 50 runs for each model. We calculated the log-likelihood using *∂a∂i*'s optimized parameter values comparing the expected and observed SFSs. For each model, we selected the maximum likelihood estimate from the 50 runs and used AIC to compare across models. We then used a mutation rate of 7e-9 mutations/site/generation and the total sequence length ( $L$ ) to calculate the diploid ancestral effective population size as  $N_{anc} = \Theta / (4 * \mu * L)$ . We scaled other inferred population size parameters by  $N_{anc}$  and time parameters by  $2 * N_{anc}$  in order to obtain values in units of diploids and numbers of generations.

### Simulations of Deleterious Genetic Variation

We performed forward-in-time genetic simulations using SLiM v3.6 (Haller and Messer 2019). We simulated a 25 Mb chromosomal segment with randomly generated introns, exons, and intergenic regions following the approach from Mooney et al. (2018). Exons comprised ~1% of the total chromosome, thus each segment contained ~0.25 Mb of coding sequence. Deleterious (nonsynonymous) mutations occurred in exonic regions at a ratio of 2.31:1 to neutral (synonymous) mutations (Huber et al. 2017). Selection coefficients ( $s$ ) for nonsynonymous mutations were drawn from a distribution estimated using human genetic variation data by Kim et al. (2017), consisting of a gamma distribution with mean  $s = -0.01314833$  and shape = 0.186. Additionally, we augmented this distribution such that 0.5% of deleterious mutations were recessive lethal, given that the DFE inferred by Kim et al. (2017) may underestimate the fraction of lethal mutations (Wade et al. 2022). We modeled deleterious mutations in noncoding regions assuming gamma distribution parameters estimated by Torgerson et al. (2009) consisting of a mean  $s = -0.001036043$  and shape = 0.0415. We assumed that 4% of noncoding mutations were deleterious (Huber et al. 2020) and all other noncoding mutations were neutral. For all mutations, we assumed a mutation rate of 7e-9 mutations per site per generation following Dussex et al. (2020). In addition, we assumed a uniform recombination rate of 1e-8 crossovers per bp per generation. For all simulations, we retained fixed mutations following the initial burn-in period, such that their impact on fitness was allowed to accumulate.

The dominance coefficients ( $h$ ) for nonsynonymous mutations were set to model an inverse relationship between  $h$  and  $s$ , given that highly deleterious mutations also tend to be highly recessive (Agrawal and Whitlock 2011; Huber et al. 2018). Specifically, we assumed  $h = 0.0$

for very strongly deleterious mutations ( $s < -0.1$ ),  $h = 0.01$  for strongly deleterious mutations ( $-0.1 \leq s < -0.01$ ),  $h = 0.1$  for moderately deleterious mutations ( $-0.01 \leq s < -0.001$ ), and  $h = 0.4$  for weakly deleterious mutations ( $s > -0.001$ ). For all simulations, we assumed that deleterious mutations in noncoding regions were nearly additive ( $h = 0.4$ ).

To test the sensitivity of our analysis to our assumed selection and dominance parameters, we ran simulations with a somewhat less recessive dominance distribution for nonsynonymous mutations of  $h = 0.0$  for very strongly deleterious mutations ( $s < -0.1$ ),  $h = 0.05$  for strongly deleterious mutations ( $-0.1 \leq s < -0.01$ ),  $h = 0.2$  for moderately deleterious mutations ( $-0.01 \leq s < -0.001$ ), and  $h = 0.45$  for weakly deleterious mutations ( $s > -0.001$ ). In addition, we also ran simulations under the selection and dominance parameters proposed by Kardos et al. (2021). This model assumes that deleterious mutations come from a gamma distribution with mean  $s$  of  $-0.05$  and shape = 0.5, augmented with an additional 5% of deleterious mutations being lethal. Dominance coefficients follow the relationship  $h = 0.5 \cdot \exp(-13 \cdot s)$ ; however, we simplified this to five dominance partitions for computational efficiency:  $h = 0.48$  for  $s \geq -0.01$ ,  $h = 0.31$  for  $-0.1 \leq s < -0.01$ ,  $h = 0.07$  for  $-0.4 \leq s < -0.1$ ,  $h = 0.001$  for  $-1.0 \leq s < -0.4$ , and  $h = 0.0$  for  $s = -1.0$ . Note that we applied these model parameters only to nonsynonymous mutations and retained the same parameters for noncoding deleterious mutations as described above. All sensitivity analyses described above were done under a model including a severe founder event for Isle Royale with bottleneck parameters  $N_e = \{2, 8, 32\}$ .

We set the population sizes of our simulations according to our best-fit 4-epoch demographic model based on the SFS from our Minnesota moose genomes (fig. 3 and supplementary table S2, Supplementary Material online). Specifically, this model estimated an ancestral effective population size of  $N_{anc} = 6,548$  diploids, followed by expansion to  $N_1 = 79,647$  for  $T_1 = 22,628$  generations, then contraction to  $N_2 = 49$  for  $T_2 = 29$  generations, and finally expansion to  $N_3 = 193,472$  for  $T_3 = 1,179$  generations. We also ran simulations under a second 4-epoch model that had a similar log-likelihood and somewhat differing parameters of  $N_{anc} = 7,017$ ,  $N_1 = 145,662$ ,  $T_1 = 20,883$ ,  $N_2 = 218$ ,  $T_2 = 142$ ,  $N_3 = 105,531$ , and  $T_3 = 1,223$ . In both cases, we allowed the ancestral population to reach mutation-selection-drift equilibrium by running a burn-in at  $N_{anc}$  for 70,000 generations.

Following the fourth epoch of both models, we added a fifth and final epoch representing the founding of the Isle Royale population, consisting of  $N_e = 187$  for 15 generations. However, when simulating under this demography, we observed that the simulated levels of inbreeding and genetic diversity for the Isle Royale population did not recapitulate those observed in our empirical data (fig. 5). Specifically, we observed only a 3.6% reduction in heterozygosity (compared to  $\sim 30\%$  in our empirical data) and an increase in  $F_{ROH}$  to just 0.08 (compared to 0.35 in our

empirical data). We hypothesized that this was due to the lack of a founder event at the origination of the Isle Royale population in our model. To explore the impact of a founder event, we modified the effective population sizes during the first three generations of the Isle Royale population, using three plausible bottleneck parameters of  $N_e = \{6, 24, 96\}$ ,  $N_e = \{4, 16, 64\}$ , and  $N_e = \{2, 8, 32\}$ . We focused on the three initial generations after founding, reflecting the period from  $\sim 1900$  to 1924 when census estimates are crude and/or unavailable (Murie 1934; Mech 1966). Specifically, little is known about the number of founding individuals, though it is likely this number was small, particularly if the population was naturally founded. Additionally, available records indicate a population size of  $\sim 300$  by 1920 and perhaps several thousand by 1930, suggesting that population growth was rapid following founding (Murie 1934; Mech 1966). Following this three-generation bottleneck, we simulated the final 12 generations at our estimated  $N_e = 187$ , representing an average effective population size for the period  $\sim 1924$ –2020 when census estimates ranged from  $\sim 500$  to 2,000 (average of  $\sim 1000$ ; Hoy, Peterson, et al. 2020).

During simulations, we recorded mean heterozygosity, mean  $F_{ROH}$  for ROH  $> 100$  kb and  $> 1$  Mb, mean genetic load (calculated multiplicatively across sites), mean inbreeding load (measured as the number of diploid lethal equivalents), and the mean number of very strongly deleterious ( $s < -0.1$ ), strongly deleterious ( $-0.1 \leq s < -0.01$ ), moderately deleterious ( $-0.01 \leq s < -0.001$ ), and weakly deleterious ( $s > -0.001$ ) alleles per individual. These quantities were estimated from a sample of 80 diploids every 1,000 generations during the burn-in, every 100 generations during the second epoch, every 5 generations during the North America founding bottleneck, every 20 generations during the fourth epoch, and every generation during the Isle Royale bottleneck. We also outputted the neutral noncoding SFS at the end of simulations from the Isle Royale population from four unrelated diploid individuals for comparison with the empirical neutral SFS from Isle Royale. For all simulated scenarios, we ran 50 replicates and averaged results across all replicates for plotting.

From the above description of our simulation model, our deleterious mutation rate per chromosome per diploid is  $U = 2 \cdot 0.25 \text{ Mb} \cdot 9 \cdot 2.31/3.31 + 2 \cdot 24.75 \text{ Mb} \cdot 9 \cdot 0.04 = 0.0163$ . This deleterious mutation rate is much lower than those typically observed genome-wide (e.g., Keightley 2012), as expected given that we are modeling a chromosomal segment 25 Mb in length. Although it is computationally intractable to simulate deleterious mutations of an entire genome, it is possible to project the simulated inbreeding load and genetic load to what would be expected for a 2.5 Gb genome, as estimated for moose (Dussex et al. 2020). For the inbreeding load, this can be done by multiplying the simulated quantity from a single 25 Mb chromosome by 100 (as inbreeding load is summed across sites), whereas for the genetic load, this can be done by exponentiating the quantity from a single chromosome to the power of 100 (as genetic load is multiplied across sites).

However, note that this assumes no linkage between 25 Mb chromosomal segments. This procedure yields a total deleterious mutation rate per diploid genome of  $U = 1.63$ , in good agreement with estimates in humans (Keightley 2012).

## Supplementary material

Supplementary data are available at *Molecular Biology and Evolution* online.

## Acknowledgments

This manuscript is dedicated to the memory of Robert Wayne in honor of his many contributions to mammalian evolutionary and conservation genetics. We are grateful to members of the Wayne and Lohmueller labs for helpful input on this work and to two anonymous reviewers for constructive feedback on our manuscript. We thank Michelle Carstensen and the Minnesota Department of Natural Resources for providing tissue samples used in this study. C.C.K. and K.E.L. were supported by the National Institutes of Health (R35GM119856 to K.E.L.). A.C.B. was supported by the National Institutes of Health Biological Mechanisms of Healthy Aging Training Program (T32AG066574). This work was supported by the National Science Foundation (DEB Small Grant #1556705 to R.K.W. and DEB-1453041 to J.A.V.), Isle Royale National Park (CESU Task Agreement No. P22AC00193-00 to S.R.H.), and a McIntire-Stennis Grant (USDA-Nifa#1014575 to J.A.V.).

## Data Availability

All scripts are available at [https://github.com/ckyrizis/moose\\_WGS\\_project](https://github.com/ckyrizis/moose_WGS_project) and raw sequence data are available in the Sequence Read Archive under BioProject PRJNA827797.

## Author Contributions

C.C.K., R.K.W., and K.E.L. conceived the study. K.E.B., J.A.V., L.M.V., S.R.H., and R.O.P. acquired samples. C.C.K. conducted all analyses with input from A.C.B. and K.E.L. and wrote the manuscript with input from all authors. R.K.W. and K.E.L. jointly supervised this work.

## References

- Adams JR, Vucetich LM, Hedrick PW, Peterson RO, Vucetich JA. 2011. Genomic sweep and potential genetic rescue during limiting environmental conditions in an isolated wolf population. *Proc R Soc B Biol Sci* **278**:3336–3344.
- Agarwal I, Fuller ZL, Myers S, Przeworski M. 2022. Relating pathogenic loss-of function mutations in humans to their evolutionary fitness costs. *eLife* **12**:e83172.
- Agarwal AF, Whitlock MC. 2011. Inferences about the distribution of dominance drawn from yeast gene knockout data. *Genetics* **187**:553–566.
- Arunkumar R, Ness RW, Wright SI, Barrett SCH. 2015. The evolution of selfing is accompanied by reduced efficacy of selection and purging of deleterious mutations. *Genetics* **199**:817–829.
- Bertorelle G, Raffini F, Bosse M, Bortoluzzi C, Iannucci A, Trucchi E, Morales HE, van Oosterhout C. 2022. Genetic load: genomic estimates and applications in non-model animals. *Nat Rev Genet* **23**:492–503.
- Broders HG, Mahoney SP, Montevecchi WA, Davidson WS. 1999. Population genetic structure and the effect of founder events on the genetic variability of moose, *Alces alces*, in Canada. *Mol Ecol* **8**:1309–1315.
- Camacho C, Coulouris G, Avagyan V, Ma N, Papadopoulos J, Bealer K, Madden TL. 2009. BLAST+: architecture and applications. *BMC Bioinformatics* **10**:421.
- Cassa CA, Weghorn D, Balick DJ, Jordan DM, Nusinow D, Samocha KE, O'Donnell-Luria A, MacArthur DG, Daly MJ, Beier DR, et al. 2017. Estimating the selective effects of heterozygous protein-truncating variants from human exome data. *Nat Genet* **49**:806–810.
- Charlesworth D, Willis JH. 2009. The genetics of inbreeding depression. *Nat Rev Genet* **10**:783–796.
- Cooper GM, Shendure J. 2011. Needles in stacks of needles: finding disease-causal variants in a wealth of genomic data. *Nat Rev Genet* **12**:628–640.
- Danecek P, Auton A, Abecasis G, Albers CA, Banks E, DePristo MA, Handsaker RE, Lunter G, Marth GT, Sherry ST, et al. 2011. The variant call format and VCFtools. *Bioinformatics* **27**:2156–2158.
- Day SB, Bryant EH, Meffert LM. 2003. The influence of variable rates of inbreeding on fitness, environmental responsiveness, and evolutionary potential. *Evolution (N. Y.)* **57**:1314–1324.
- Decesare NJ, Weckworth B V, Pilgrim KL, Walker ABD, Bergman EJ, Colson KE, Corrigan R, Harris RB, Hebblewhite M, Jesmer BR, et al. 2020. Phylogeography of moose in western North America. *J Mammal* **101**:10–23.
- Dussex N, Alberti F, Heino MT, Olsen R-A, van der Valk T, Ryman N, Laikre L, Ahlgren H, Askeyev IV, Askeyev OV, et al. 2020. Moose genomes reveal past glacial demography and the origin of modern lineages. *BMC Genomics* **21**:1–13.
- Dussex N, van der Valk T, Morales HE, Wheat CW, Díez-del-Molino D, von Seth J, Foster Y, Kutschera VE, Guschanski K, Rhie A, et al. 2021. Population genomics of the critically endangered kākāpō. *Cell Genomics* **1**:100002.
- Estes JA, Terborgh J, Brashares JS, Power ME, Berger J, Bond WJ, Carpenter SR, Essington TE, Holt RD, Jackson JBC, et al. 2011. Trophic downgrading of planet earth. *Science* **333**:301–306.
- Frankham R. 1995. Effective population size/adult population size ratios in wildlife: a review. *Genet Res Cambridge* **66**:95–107.
- Fuller ZL, Berg JJ, Mostafavi H, Sella G, Przeworski M. 2019. Measuring intolerance to mutation in human genetics. *Nat Genet* **51**:772–776.
- Gaillard J-M. 2007. Are moose only a large deer?: some life history considerations. *Alces* **43**:1–12.
- Gibson AK, Nguyen AE. 2021. Does genetic diversity protect host populations from parasites? A meta-analysis across natural and agricultural systems. *Evol. Lett.* **5**:16–32.
- Glémin S. 2003. How are deleterious mutations purged? Drift versus nonrandom mating. *Evolution (N. Y.)* **57**:2678–2687.
- Grossen C, Guillaume F, Keller LF, Croll D. 2020. Purging of highly deleterious mutations through severe bottlenecks in Alpine ibex. *Nat Commun* **11**:1001.
- Gutenkunst RN, Hernandez RD, Williamson SH, Bustamante CD. 2009. Inferring the joint demographic history of multiple populations from multidimensional SNP frequency data. *PLoS Genet* **5**:1–11.
- Haddad NM, Brudvig LA, Clobert J, Davies KF, Gonzalez A, Holt RD, Lovejoy TE, Sexton JO, Austin MP, Collins CD, et al. 2015. Habitat fragmentation and its lasting impact on Earth's Ecosystems. *Sci Adv* **1**:1–10.
- Haller BC, Messer PW. 2019. SLim 3: forward genetic simulations beyond the Wright-Fisher model. *Mol Biol Evol* **36**:632–637.

- Hedrick PW. 1994. Purging inbreeding depression and the probability of extinction: full-sib mating. *Heredity (Edinb)*. **73**:363–372.
- Hedrick PW, Garcia-Dorado A. 2016. Understanding inbreeding depression, purging, and genetic rescue. *Trends Ecol Evol*. **31**:940–952.
- Hedrick PW, Robinson JA, Peterson RO, Vucetich JA. 2019. Genetics and extinction and the example of Isle Royale wolves. *Anim Conserv*. **22**:302–309.
- Hoy SR, MacNulty DR, Smith DW, Stahler DR, Lambin X, Peterson RO, Ruprecht JS, Vucetich JA. 2020. Fluctuations in age structure and their variable influence on population growth. *Funct Ecol*. **34**:203–216.
- Hoy SR, Peterson RO, Vucetich JA. 2020. *Ecological studies of wolves on Isle Royale. Annual report 2019–2020*. Houghton, MI: Michigan Technological University.
- Huber CD, Durvasula A, Hancock AM. 2018. Gene expression drives the evolution of dominance. *Nat Commun*. **9**:1–11.
- Huber CD, Kim BY, Lohmueller KE. 2020. Population genetic models of GERP scores suggest pervasive turnover of constrained sites across mammalian evolution. *PLoS Genet*. **16**:1–26.
- Huber CD, Kim BY, Marsden CD, Lohmueller KE. 2017. Determining the factors driving selective effects of new nonsynonymous mutations. *Proc Natl Acad Sci U S A*. **114**:4465–4470.
- Hundertmark KJ, Bowyer RT, Shields GF, Schwartz CC. 2003. Mitochondrial phylogeography of moose (*Alces alces*) in North America. *J Mammal*. **84**:718–728.
- Hundertmark KJ, Shields GF, Udina IG, Bowyer RT, Danilkin AA, Schwartz CC. 2002. Mitochondrial phylogeography of moose (*Alces alces*): Late Pleistocene divergence and population expansion. *Mol Phylogenet Evol*. **22**:375–387.
- Kalbfleisch TS, Murdoch BM, Smith TPL, Murdoch JD, Heaton MP, McKay SD. 2018. A SNP resource for studying North American moose. *F1000Res*. **7**:1–17.
- Kardos M, Armstrong EE, Fitzpatrick SW, Hauser S, Hedrick PW, Miller JM, Tallmon DA, Chris Funk W. 2021. The crucial role of genome-wide genetic variation in conservation. *Proc Natl Acad Sci U S A*. **118**:1–10.
- Keightley PD. 2012. Rates and fitness consequences of new mutations in humans. *Genetics*. **190**:295–304.
- Keller L, Waller DM. 2002. Inbreeding effects in wild populations. *Trends Ecol Evol*. **17**:19–23.
- Khan A, Patel K, Shukla H, Viswanathan A, van der Valk T, Borthakur U, Nigam P, Zachariah A, Jhala Y V, Kardos M, et al. 2021. Genomic evidence for inbreeding depression and purging of deleterious genetic variation in Indian tigers. *Proc Natl Acad Sci U S A*. **118**:1–10.
- Kim BY, Huber CD, Lohmueller KE. 2017. Inference of the distribution of selection coefficients for new nonsynonymous mutations using large samples. *Genetics*. **206**:345–361.
- Kirin M, McQuillan R, Franklin CS, Campbell H, Mckeigue PM, Wilson JF. 2010. Genomic runs of homozygosity record population history and consanguinity. *PLoS ONE*. **5**:1–7.
- Kirkpatrick M, Jarne P. 2000. The effects of a bottleneck on inbreeding depression and the genetic load. *Am Nat*. **155**:154–167.
- Kleinman-Ruiz D, Lucena-Perez M, Villanueva B, Fernandez J, Saveljev AP, Ratkiewicz M, Schmidt K, Galtier N, Garcia-Dorado A, Godoy JA. 2022. Purging of deleterious burden in the endangered Iberian lynx. *Proc Natl Acad Sci U S A*. **119**:1–11.
- Kyriazis CC, Robinson JA, Lohmueller KE. 2022. Using computational simulations to quantify genetic load and predict extinction risk. *bioRxiv* doi: 10.1101/2022.08.12.503792.
- Kyriazis CC, Wayne RK, Lohmueller KE. 2021. Strongly deleterious mutations are a primary determinant of extinction risk due to inbreeding depression. *Evol Lett*. **5**:33–47.
- Li H. 2013. Aligning sequence reads, clone sequences and assembly contigs with BWA-MEM. *arXiv:1303.3997v2 [Internet]* **00**:1–3. Available from: <http://arxiv.org/abs/1303.3997>
- MacArthur D, Balasubramanian S, Frankish A. 2012. A systematic survey of loss-of-function variants in human protein-coding genes. *Science*. **335**:1–14.
- MacArthur DG, Tyler-Smith C. 2010. Loss-of-function variants in the genomes of healthy humans. *Hum Mol Genet*. **19**:125–130.
- Manichaikul A, Mychaleckyj JC, Rich SS, Daly K, Sale M, Chen WM. 2010. Robust relationship inference in genome-wide association studies. *Bioinformatics*. **26**:2867–2873.
- McLaren W, Gil L, Hunt SE, Riat HS, Ritchie GRS, Thormann A, Flicek P, Cunningham F. 2016. The ensembl variant effect predictor. *Genome Biol*. **17**:1–14.
- McLaren BE, Peterson RO. 1994. Wolves, moose, and tree rings on Isle Royale. *Science*. **266**:1555–1558.
- McVean G. 2009. A genealogical interpretation of principal components analysis. *PLoS Genet*. **5**:e1000686.
- Mech LD. 1966. The Wolves of Isle Royale.
- Mooney JA, Huber CD, Service S, Sul JH, Marsden CD, Zhang Z, Sabatti C, Ruiz-Linares A, Bedoya G, Endophenotypes C 5 RC for GI of B, et al. 2018. Understanding the hidden complexity of Latin American population isolates. *Am J Hum Genet*. **103**:707–726.
- Murie A. 1934. Moose of Isle Royale. *Univ Michigan Museum Zool Misc Publ*. **25**:1–44.
- Murray DL, Cox EW, Ballard WB, Whitlaw HA, Lenarz MS, Custer TW, Barnett T, Fuller TK. 2006. Pathogens, nutritional deficiency, and climate influences on a declining moose population. *Wildl Monogr*. **166**:1–30.
- Narasimhan V, Danecek P, Scally A, Xue Y, Tyler-Smith C, Durbin R. 2016. BCFtools/ROH: a hidden Markov model approach for detecting autozygosity from next-generation sequencing data. *Bioinformatics*. **32**:1749–1751.
- Nietlisbach P, Muff S, Reid JM, Whitlock MC, Keller LF. 2019. Nonequivalent lethal equivalents: models and inbreeding metrics for unbiased estimation of inbreeding load. *Evol Appl*. **12**:266–279.
- Pedersen CET, Lohmueller KE, Grarup N, Bjerregaard P, Hansen T, Siegmund HR, Moltke I, Albrechtsen A. 2017. The effect of an extreme and prolonged population bottleneck on patterns of deleterious variation: insights from the Greenlandic Inuit. *Genetics*. **205**:787–801.
- Pekkala N, Knott KE, Kotiaho JS, Puurtinen M. 2012. Inbreeding rate modifies the dynamics of genetic load in small populations. *Ecol Evol*. **2**:1791–1804.
- Pérez-Pereira N, Caballero A, García-Dorado A. 2022. Reviewing the consequences of genetic purging on the success of rescue programs. *Conserv Genet*. **23**:1–17.
- Pérez-Pereira N, Pouso R, Rus A, Vilas A, López-Cortegano E, García-Dorado A, Quesada H, Caballero A. 2021. Long-term exhaustion of the inbreeding load in *Drosophila melanogaster*. *Heredity (Edinb)*. **127**:373–383.
- Räikkönen J, Vucetich JA, Peterson RO, Nelson MP. 2009. Congenital bone deformities and the inbred wolves (*Canis lupus*) of Isle Royale. *Biol Conserv*. **142**:1025–1031.
- Raj A, Stephens M, Pritchard JK. 2014. FastSTRUCTURE: variational inference of population structure in large SNP data sets. *Genetics*. **197**:573–589.
- Ralls K, Sunnucks P, Lacy RC, Frankham R. 2020. Genetic rescue: a critique of the evidence supports maximizing genetic diversity rather than minimizing the introduction of putatively harmful genetic variation. *Biol Conserv*. **251**:108784.
- R Core Team. 2021. R: A language and environment for statistical computing. Available from: <https://www.r-project.org/>
- Ripple WJ, Estes JA, Beschta RL, Wilmers CC, Ritchie EG, Hebblewhite M, Berger J, Elmhagen B, Letnic M, Nelson MP, et al. 2014. Status and ecological effects of the world's largest carnivores. *Science*. **343**:1–11.
- Robinson JA, Brown C, Kim BY, Lohmueller KE, Wayne RK. 2018. Purging of strongly deleterious mutations explains long-term persistence and absence of inbreeding depression in island foxes. *Curr Biol*. **28**:3487–3494.e4.
- Robinson JA, Kyriazis CC, Nigenda-Morales SF, Beichman AC, Rojas-Bracho L, Robertson KM, Fontaine MC, Wayne RK, Lohmueller KE, Taylor BL, et al. 2022. The critically endangered vaquita is not doomed to extinction by inbreeding depression. *Science*. **639**:635–639.



- Robinson J, Kyriazis CC, Yuan SC, Lohmueller KE. 2023. Deleterious variation in natural populations and implications for conservation genetics. *Annu Rev Anim Biosci*. doi: 10.1146/annurev-animal-080522-093311.
- Robinson JA, Rääkkönen J, Vucetich LM, Vucetich JA, Peterson RO, Lohmueller KE, Wayne RK. 2019. Genomic signatures of extensive inbreeding in Isle Royale wolves, a population on the threshold of extinction. *Sci Adv*. **5**:1–13.
- Ruprecht JS, Hersey KR, Hafen K, Monteith KL, Decesare NJ, Kauffman MJ, Macnulty DR. 2016. Reproduction in moose at their southern range limit. *J Mammal*. **97**:1355–1365.
- Sandell L, Sharp NP. 2022. Fitness effects of mutations: an assessment of PROVEAN predictions using mutation accumulation data. *Genome Biol. Evol.* **14**:1–15.
- Sattler RL, Willoughby JR, Swanson BJ. 2017. Decline of heterozygosity in a large but isolated population: a 45-year examination of moose genetic diversity on Isle Royale. *PeerJ*. **5**:1–18.
- Simons YB, Turchin MC, Pritchard JK, Sella G. 2014. The deleterious mutation load is insensitive to recent population history. *Nat Genet*. **46**:220–224.
- Stoffel MA, Johnston SE, Pilkington JG, Pemberton JM. 2021a. Mutation load decreases with haplotype age in wild Soay sheep. *Evol Lett*. **5**:187–195.
- Stoffel MA, Johnston SE, Pilkington JG, Pemberton JM. 2021b. Genetic architecture and lifetime dynamics of inbreeding depression in a wild mammal. *Nat Commun*. **12**:1–10.
- Swinford NA, Prall SP, Williams CM, Sheehama J, Scelza BA, Henn BM. 2022. Increased homozygosity due to endogamy results in fitness consequences in a human population. *bioRxiv*. doi: 10.1101/2022.07.25.501261.
- Szpiech ZA, Mak ACY, White MJ, Hu D, Eng C, Burchard EG, Hernandez RD. 2019. Ancestry-dependent enrichment of deleterious homozygotes in runs of homozygosity. *Am J Hum Genet*. **105**:747–762.
- Szpiech ZA, Xu J, Pemberton TJ, Peng W, Zöllner S, Rosenberg NA, Li JZ. 2013. Long runs of homozygosity are enriched for deleterious variation. *Am J Hum Genet*. **93**:90–102.
- Teixeira JC, Huber CD. 2021. The inflated significance of neutral genetic diversity in conservation genetics. *Proc Natl Acad Sci U S A*. **118**:1–10.
- Timmermann HR, Rodgers AR. 2017. The status and management of moose in North America—circa 2015. *Alces A J Devoted to Biol Manag Moose*. **53**:1–22.
- Torgerson DG, Boyko AR, Hernandez RD, Indap A, Hu X, White TJ, Sninsky JJ, Cargill M, Adams MD, Bustamante CD, et al. 2009. Evolutionary processes acting on candidate cis-regulatory regions in humans inferred from patterns of polymorphism and divergence. *PLoS Genet*. **5**:e1000592.
- Van der Auwera GA, Carneiro MO, Hartl C, Poplin R, del Angel G, Levy-Moonshine A, Jordan T, Shakir K, Roazen D, Thibault J, et al. 2013. From fastQ data to high-confidence variant calls: the genome analysis toolkit best practices pipeline. *Curr Protoc Bioinformatics*. **43**:11.10.1–11.10.33.
- Vaser R, Adusumalli S, Leng SN, Sikic M, Ng PC. 2016. SIFT Missense predictions for genomes. *Nat Protoc*. **11**:1–9.
- Vucetich JA. 2021. *Restoring the balance: what wolves tell us about our relationship with nature*. Baltimore, MD: Johns Hopkins Press.
- Wade EE, Kyriazis CC, Cavassim MIA, Lohmueller KE. 2022. Quantifying the fraction of new mutations that are recessive lethal. *bioRxiv*. doi: 10.1101/2022.04.22.489225.
- Wang J, Hill WG, Charlesworth D, Charlesworth B. 1999. Dynamics of inbreeding depression due to deleterious mutations in small populations: mutation parameters and inbreeding rate. *Genet Res*. **74**:165–178.
- Weir BS, Cockerham CC. 1984. Estimating F-statistics for the analysis of population structure. *Evolution (N. Y.)*. **38**:1358–1370.
- Wilson PJ, Grewal S, Rodgers A, Rempel R, Saquet J, Hristienko H, Burrows F, Peterson R, White BN. 2003. Genetic variation and population structure of moose (*Alces alces*) at neutral and functional DNA loci. *Can J Zool*. **683**:670–683.
- Wolfe ML, Hersey KR, Stoner DC. 2010. A history of moose management in Utah. *Alces A J Devoted to Biol Manag Moose*. **46**:37–52.
- Xue Y, Prado-Martinez J, Sudmant PH, Narasimhan V, Ayub Q, Szpak M, Frandsen P, Chen Y, Yngvadottir B, Cooper DN, et al. 2015. Mountain gorilla genomes reveal the impact of long-term population decline and inbreeding. *Science*. **348**:242–245.
- Zheng X, Levine D, Shen J, Gogarten S, Laurie C, Weir B. 2012. A high-performance computing toolset for relatedness and principal component analysis of SNP data. *Bioinformatics*. **28**:3326–3328.